Materials Physics and Mechanics 47 (2021) 582-591 Received: July 10, 2020
Research article

EFFECT OF TRACE IMPURITIES ON THE THERMOELECTRIC PROPERTIES OF COMMERCIALLY PURE ALUMINUM

M.S. Kaiser*

Directorate of Advisory, Extension and Research Services, Bangladesh University of Engineering and Technology, Dhaka-1000, Bangladesh

*e-mail: mskaiser@iat.buet.ac.bd

Abstract. Impurities play an important role in the properties of aluminum. Those are incorporated into commercially pure aluminum through repeated melting and samples are characterized for their thermal conductivity, dielectric and morphological properties as a function of cold deformation and annealing temperature. Results indicate that cold rolling increases thermal conductivity since reduces the porosity like defects but heavily cold-working decreases the conductivity because of distorts the crystal lattice. Material defects are more prominent than impurities in the material in the case of AC electrical properties. The dielectric constant and loss tangent decreases with annealing temperature initially due to stress reliving and increases due to the formation of metastable phases. Trace added alloys show more eutectic silicon and other Fe-rich intermetallic phases into the microstructure.
Keywords: aluminum, impurities, conductivity, dielectric, microstructure

.

1. Introduction

Commercial pure aluminum is an essential conductive material that is well known for good electrical conductivity. Some mechanical treatments can improve its strength furtherer without any difficulty [1,2]. Aluminum shows about 61 percent of the electrical conductivity of copper where it contains only 30 percent of the weight of copper. Thus, in the case of containing the same electrical resistance, a bare wire of aluminum weighs half as much as a bare wire of copper. Nowadays aluminum is used as an electrical conductor universally. In developing countries, the use of copper is substituted with aluminum to save foreign exchange by reducing copper imports. The reason behind choosing aluminum is for its easy availability, lower and steady price, conductivity, and adequate physical properties [3,4]. During the casting of aluminum, exogenous inclusions may evolve from the melting environment for example the refractory linings of furnaces, ladles, reactors, or launders, etc. [5,6]. Oxide films and intermetallic particles are considered to be the two most prominent types of impurities in aluminum. The incorporation of these two can adversely affect the mechanical, electrical, physical, and chemical properties of aluminum castings, for example, the strengths, electrical and thermal conductivities, and corrosion resistance, and so on [7-9]. Technically, iron, and silicon exist as the main impurities in pure aluminum. Generally, all commercial wrought aluminum alloys have at least some amount of iron and silicon and the growing concentration is caused by increasing use of recycled aluminum in manufacturing [10]. Because of dislocation or grain-boundary pinning, the formation of intermetallic phases in an aluminum matrix contains a strengthening effect [11].

In this research, an analysis has been carried out to assess the repeated melting influence upon the thermal and the AC electrical properties of commercially pure aluminum.

© M.S. Kaiser, 2021. Peter the Great St. Petersburg Polytechnic University
This is an open access article under the CC BY-NC 4.0 license (https://creativecommons.org/li-censes/by-nc/4.0/)

2. Materials and methods

A clay-graphite crucible in a natural gas-fired pit furnace was used for melting these experimental alloys. During melting suitable flux cover like degasser, borax, etc was used. The melting temperature was always maintained at 780±15°C with the help of an electronic controller. Preparation of the alloys the 99.80 wt% purity commercially pure aluminum was taken as the starting material Alloy 1. First, the commercially pure aluminum was melted in the clay-graphite crucible idiom as Alloy 2, and then it was remelted again for preparing Alloy 3. Casting was done in mild steel metal mould of size 17.0×51.0×200.0 in millimeter. The mould was coated inside with a film of water-clay and was preheated at 250°C. Then the homogenized melts under stirring at 700°C were poured in that preheated mould. A shaper machine was used to skin out the oxide layer from the cast surfaces. The chemical composition of the investigated alloys was determined by optical emission spectroscopy as listed in Table 1. The cast alloys were homogenized at a temperature of 450°C for 12 hours to redistribute the precipitating element(s) evenly through the part. The solid solution treatments were carried out at 525°C for two hours and then water was quenched to room temperature to get a supersaturated single-phase region. Cold rolling of the cast alloys at different reduction percentages was carried out in a 10HP capacity rolling mill. The sample sizes were 16×16×50 mm and thickness reduction was given per pass about 1.0 mm. Samples for the studying electrical conductivity and alternating current measurement 4×15×15 mm and 10×10×2.5 mm in size respectively were obtained from the cast and various cold-rolled samples. The finished surface samples produced by grinding and polishing were prepared for these measurements. Cold rolled samples were annealed isochronally for 60 minutes at different temperatures up to 400°C. Electrical conductivity of the alloys was carried out with an Electric Conductivity Meter, type 979. Thermal conductivity was calculated from those electrical conductivity data through the Wiedemann–Franz law [12]. For the AC electrical measurements an LCR meter and Impedance Analyzer in the range of 100 Hz ≤ f ≤ 100 MHz was used at room temperature. The samples were modelled in parallel equivalent circuit mode for dielectric measurements. For the scanning electron micrographic (SEM) study the heat-treated samples were polished sequentially with 2000 grade grinding paper and finally with alumina followed by etched using Keller's reagent. A JEOL scanning electron microscope with an X-ray analyzer was used for this study to verify the different elements present in the experimental alloys.

Table 1. Chemical composition of the experimental alloys (wt%)

Alloy	Si	Fe	Mg	Cu	Mn	Cr	Zn	Ni	Pb	Sn	Al
1	0.0210	0.1806	0.0016	0.0022	0.0021	0.0016	0.0004	0.0000	0.0000	0.0000	Bal
2	0.4647	0.5820	0.0071	0.0091	0.0041	0.0294	0.0553	0.0175	0.0065	0.0017	Bal
3	0.8357	0.6273	0.0061	0.0150	0.0185	0.0453	0.0526	0.0195	0.0085	0.0019	Bal

3. Results and discussion

Thermal conductivity. Figure 1 shows the dependence of thermal conductivity of commercially pure aluminum Alloy 1 and the trace impurities added Alloy 2 and Alloy 3 on deformation degree after cold rolling. It can be seen that the thermal conductivity at the initial stage slowly increases with the deformation degree. Cast alloys always stuffing porosity or pinholes which produce during casting. A decrease in the porosity of cast alloys during cold rolling results in an increase in conductivity. However, heavily cold-working of the experimental alloys results in a decrease in thermal conductivity. Aluminum is a good conductor of heat because of a large number of free electrons moving about its lattice structure [13]. Like other metals, the properties of aluminum such as thermal conductivity are affected by plastic deformation [14]. Cold working usually distorts the whole crystal lattice

and makes it more difficult for electron flow into the materials [15]. It can be seen that the thermal conductivity for highly pure aluminum is higher than that for trace added alloys. The addition of impurities increases the residual resistivity of the samples which is responsible for lowering the thermal conductivity [16]. The variations of the thermal conductivity of the 75% cold-rolled alloys against isochronal annealing are shown in Fig. 2. During annealing, the initial increase in conductivity are due to the stress-relieving and dislocation rearrangement in the alloys. The final steady increase in conductivity at higher annealing temperature appears from particle coarsening which reduces the number of scattering centers. Since precipitate coarsening as well as recovery and recrystallization are appreciable at high annealing temperatures, the conductivity raise is noticeable. At the intermediate stage of annealing, the subsequent decrees in conductivity are due to the appearance of fine precipitation of metastable phases.

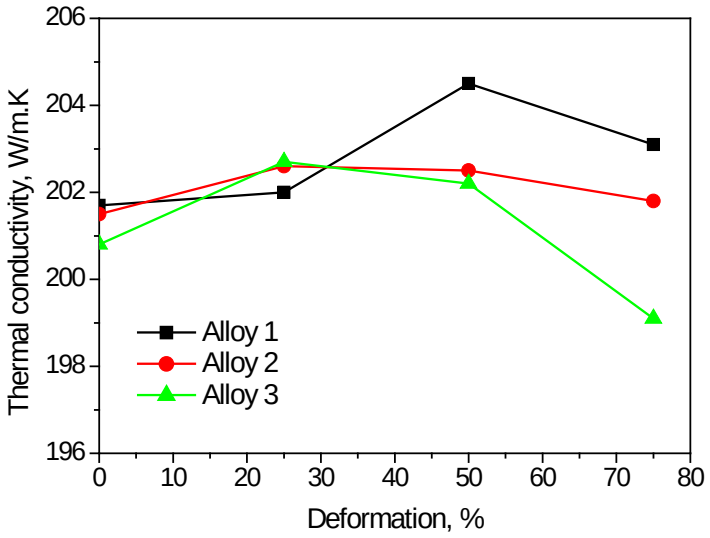

Fig. 1. Variation of the thermal conductivity with percentage deformation

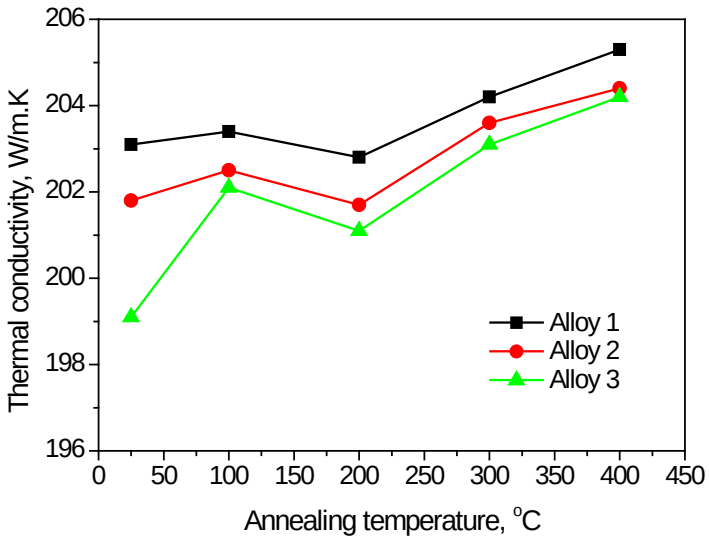

Fig. 2. Variation of thermal conductivity with annealing temperature

Dielectric properties. The frequency dependence of the impedance behaviour of impurities incorporated in different cast alloys at room temperature can be seen in Fig. 3. It has been observed that all of the samples exhibited relatively high impedance at low frequencies and it decreased with increasing the frequency. In conformity with Drude Lorentz

model, at lower frequencies, capacitive impacts are elevated due to there being the dispersive effect of the electrons colliding with the lattice as well as electric polarization of the bound electrons not in the conduction band. Some interfacial polarization effects may also have appeared. This leads to the high impedance at lower frequencies as it is a combination of both the capacitive and purely resistive effects [17]. From the graph, it is shown that commercially pure aluminum attain the highest impedance followed the trace added alloys. The impedance of a material depends on the impurities, microstructural defects, grain boundaries, porosity, microcracks, crystallite orientation, dislocations vacancies, dopant atoms, etc. Normally addition of impurities significantly increases the impedance characteristics of the metal. But cast alloys contents porosity, microcracks, etc. like defects that increase the impedance. In these cases, it is more prominent of the cast materials [18].

Figure 4 shows the changing of the impedance of aluminum samples at 10^3 Hz frequency with respect to the degree of deformation. From the graph, it is seen that sometimes the impedance increases or decreases with percentages of deformation. The decreases of impedance with deformation degree are the results of a decrease in the porosity during cold rolling. However, cold-working interactions of solute atoms with lattice defects such as dislocations, vacancies, and stacking faults introduced during rolling, may also cause a considerable increase in impedance.

The results of the impedance at 10^3 Hz frequency due to isochronal annealing of the 75% cold-rolled samples at different temperatures for 1 hour are shown in Fig. 5. At room temperature impedance is seen to be lower. While isochronal annealing is done, at the initial stage two things have happened. Dislocation rearrangement has occurred into the cold-rolled alloys cause the decrease in impedance and formation of fine intermetallic precipitates cause the increase in impedance. Combined of these effects reflect the overall intensity of impedance. When the samples are annealed at a higher temperature, an increase in impedance is noted due to grain growth. The overall intensity of impedance is lower for commercially pure aluminum Alloy 1 than Alloy 2 and 3 due to the presence of lower impurities in the material. Impurities barrier in the path which inhibits the movement of electrons as a result of the higher impedance [19].

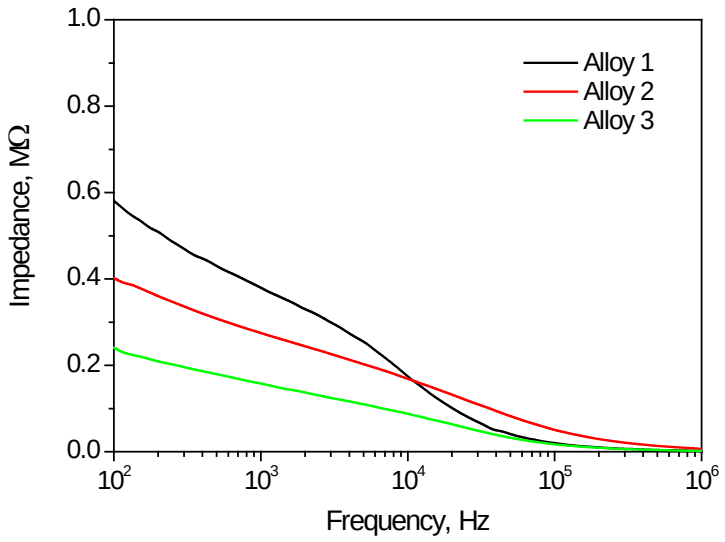

Fig. 3. Impedance behaviour of the alloys as a function of the applied frequency

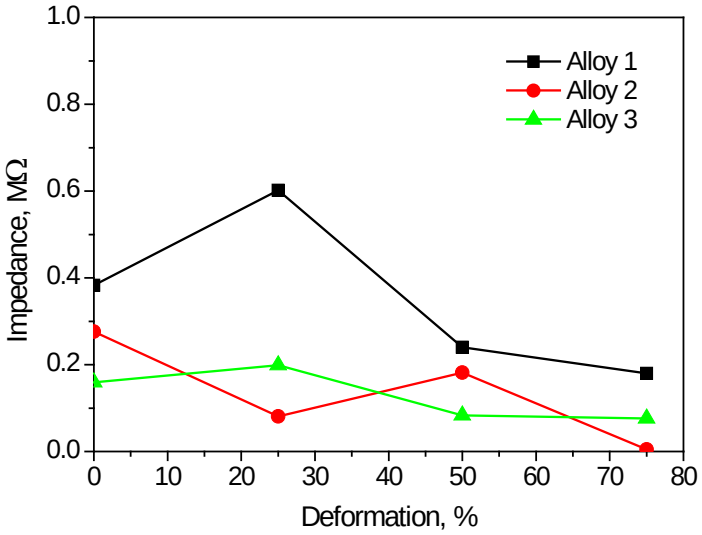

Fig. 4. Behaviour of the impedance with percentage deformation at 10^3 Hz frequency

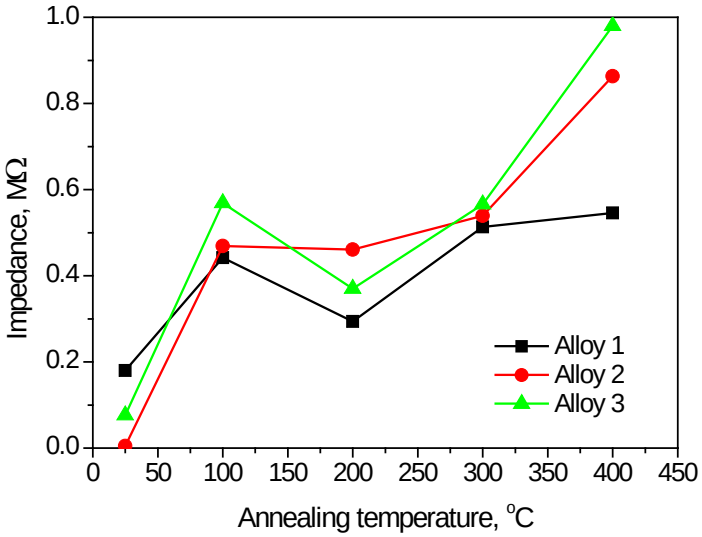

Fig. 5. Variation of thermal conductivity with annealing temperature

The dielectric constant of the cast alloys was measured at room temperature over the frequency range of 10^2 Hz to 10^6 Hz, as shown in Fig. 6. It is observed that the dielectric constant decreases with an increase in the frequency of an applied field. The decrease in the values of dielectric constant with an increase of frequency can be related to the diminution of space charge polarization effect. However, the initially dielectric constant is high because of the appearance of space charge polarization at grain boundaries, which creates an effective barrier. Further, with the increase of frequency, the dielectric constant decreases which can be clarified by the dipole relaxation phenomenon. More often the electrons reverse their movement direction as the frequency increases, which lessens the feasibility of electrons reaching grain boundary, thus, polarization reduces. As a result, with the thriving frequency of the applied field, the dielectric constant decreases eventually and remains nearly constant [20].

It is also found that melted aluminum Alloy 2 provides a higher dielectric constant than commercially pure aluminum Alloy 1, while re-melted Alloy 3 shows a maximum dielectric constant. This phenomenon occurs because melted aluminum contains impurities and various types of intermetallic, as well as the dominance of grain boundary, affects the dielectric constant to a higher rate ultimately.

Figure 7 shows the variation of dielectric constant at room temperature with respect to rolling deformation for 10^3 Hz frequency. As elongated grains are formed and more grain boundaries are generated. Therefore, the dielectric constant reduces. With the rise of rolling deformation dislocation density increases and a serious change of grain orientation takes place causes the increase of the dielectric constant. The trace-added alloys accelerate the increment of the dielectric constant. Transition metals are known to strongly bind the vacancies causes a rise in the dielectric constant [11].

From Fig. 8, the cold-rolled experimental alloys at 10^3 Hz frequency, the dielectric constant indicates irregularities with annealing temperature. The initial decrease of dielectric constant with increasing annealing temperature can be interpreted by the enhancement of defect-free crystal structure which was formed by cold rolling. At the low temperature of annealing, recovery takes place into the cold-rolled material through annihilation of point defects and rearrangement of dislocations. Iron and silicon are the inevitable impurities in commercial purity aluminum alloys. The precipitation reaction due to these impurities easily occurs during heat treatment. At the intermediate stage of annealing formation of fine precipitates of metastable phases causes the increase of dielectric constant of the experimental aluminum alloys. The fine precipitates hinder the electron movement into the alloys as a higher dielectric constant. Finally, it is enhanced as the grain size increases at higher annealing temperature which resulting in a reduction in the number of grain boundaries [21].

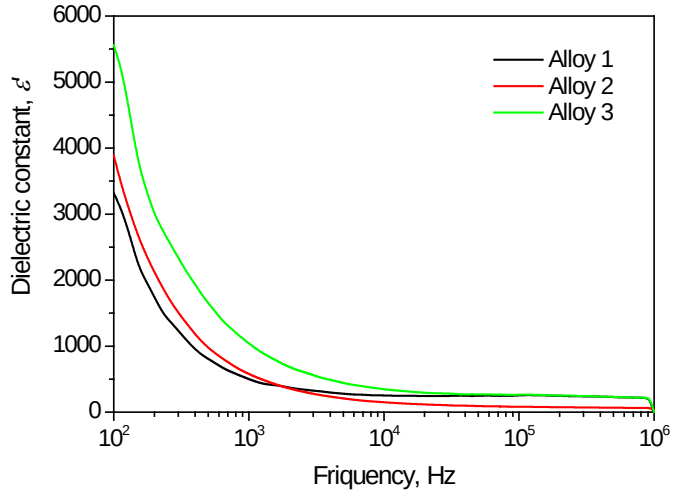

Fig. 6. Variation of the dielectric constant of the alloys as a function of the applied frequency

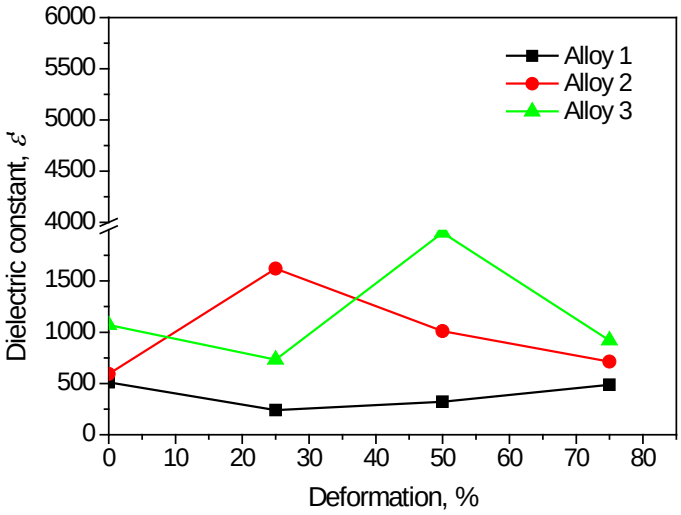

Fig. 7. Behaviour of the dielectric constant with percentage deformation at 10^3 Hz frequency

The variation of dielectric loss of the cold-rolled samples with annealing temperature at the frequency 10^3 Hz shows the similar nature of the dielectric constant as displayed in Fig. 9. It is seen that all the samples demonstrate an overall decrease in loss factor when they undergo thermal treatment at a lower temperature. The low values of dielectric loss indicate that the grain contains minimum defects through recovery. After annealing at high temperature metastable phase formation make the material defects. As a result, shows the higher values of dielectric loss. The dynamism of charge increases with temperature and enhances the polarization and eventually tends to high dielectric loss [22]. The rate of fine precipitates is higher for Alloys 2 and Alloy 3 since they content higher impurities [23].

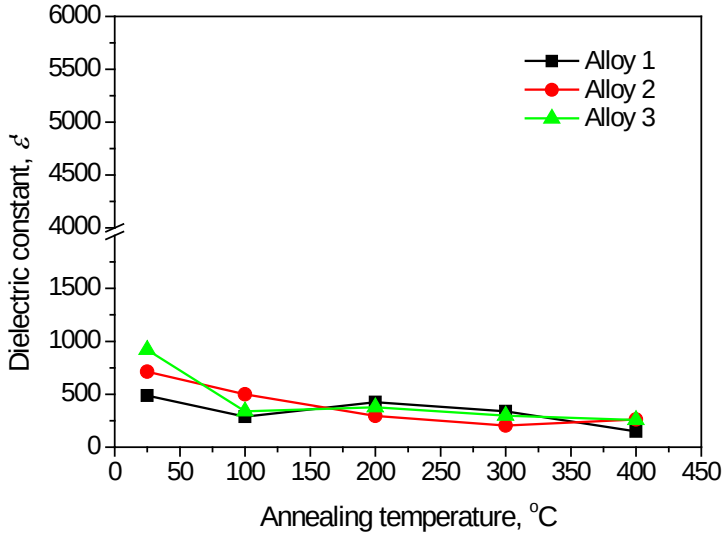

Fig. 8. Variation of the dielectric constant of experimental alloys as a function of annealing temperature at the frequency of 10^3 Hz

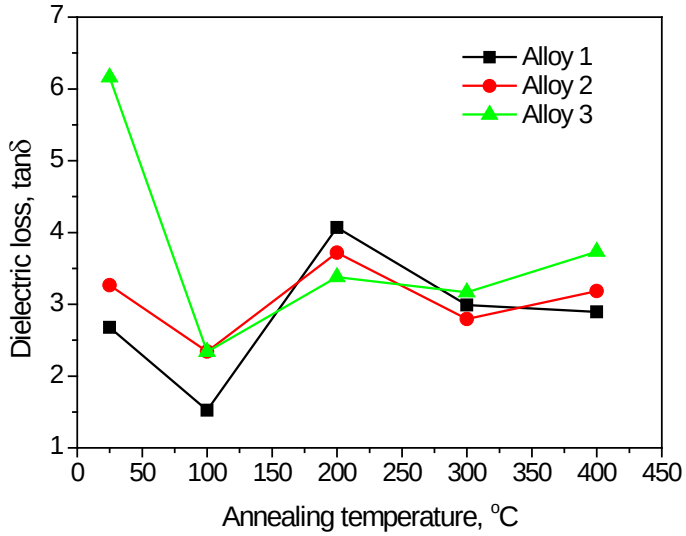

Fig. 9. Variation of dielectric loss of experimental alloys as a function of annealing temperature at the frequency of 10^3 Hz

Scanning electron microscopy. Figure 10 shows the SEM micrographs of 75% cold-rolled alloys followed by annealing at 200°C for one hour. The microstructures of all the alloys exhibit the morphology of a fine α-Al + Si eutectic mixture, eutectic silicon, and other Fe-rich intermetallic phases [24,25]. Due to the presence of higher impurities, eutectic silicon and other Fe-rich intermetallic phases are more visible in trace added alloys especially in Alloy 3. From Table 1, it is observed that Alloy 3 contains the highest percentages of Si and

Fe. The corresponding EDX of the SEM of the experimental alloys is shown in Figs. 10(a-c). The EDX scan reveals the following chemical composition by weight percentage as Alloy 1, 97.63% Al, 0.96% Si, 0.04 % Cr, 0.04 % Mn, 1.08% Fe and 0.18% Cu. Alloy 2 are 92.46% Al, 4.59% Si, 1.76% Mn, 0.67% Fe, 0.42% Cu and 0.10%Zn, and Alloy 3 are 89.94% Al, 9.05% Si, 0.23% Mn, 0.43% Fe, 0.16% Cu and 0.04% Zn. This analysis confirms that Alloy 2 shows superior impurities than Alloy 1 and the particles of the highest volume fraction presence in Alloy 3.

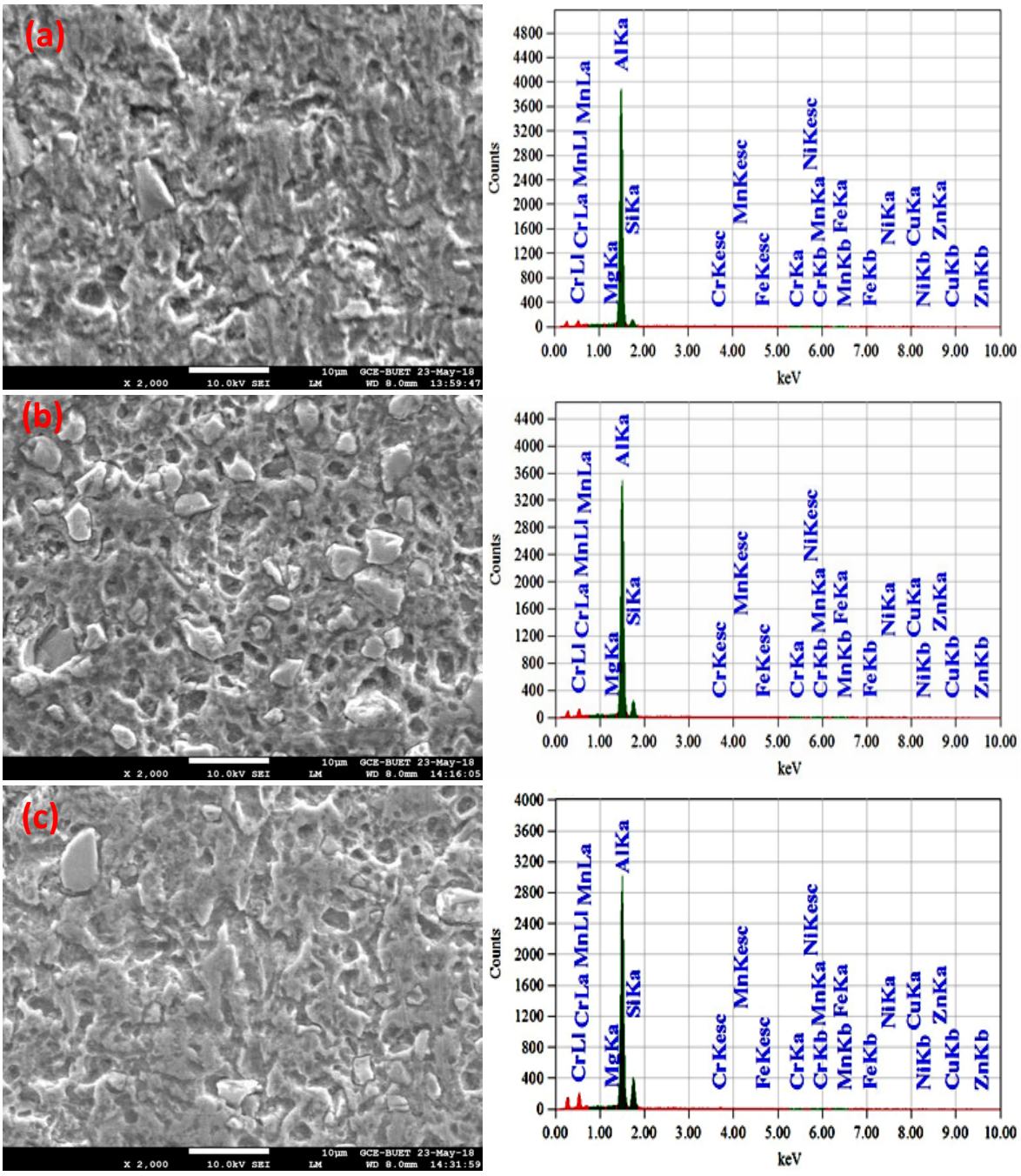

Fig. 10. SEM images and EDX analysis of 75% cold-rolled (a) Alloy 1, (b) Alloy 2 and (c) Alloy 3 aged at 200°C for one hour

4. Conclusions

In this study, thermal conductivity and the AC electrical properties of commercially pure aluminum with trace impurities like Fe, Si were investigated as a function of frequency, deformation, and temperature; the following conclusions can be obtained.

Impurities and material defects like porosity, dislocation decrease the thermal conductivity of aluminum. Cold rolling results in an increase in conductivity because of reducing in the porosity like defects but heavily cold-working results in a decrease in thermal conductivity because of distorts the crystal lattice.

Dependence of AC electrical properties as impedance is more prominent on material defects than impurities presence into the material.

Annealing at low temperature reduces the dielectric constant and loss tangent because of stress relieving as well as dislocation rearrangement and increases at higher temperature due to formation of fine precipitates metastable phases into the alloys.

The microstructures of the trace added alloys are evidence for more eutectic silicon and other Fe-rich intermetallic phases into the alloys.

Acknowledgements*. The author would like to extend his sincere appreciation to the DAERS office of Bangladesh University of Engineering and Technology, Dhaka-1000 for all kinds of support. Use of laboratory facilities at Department of Glass and Ceramics Engineering is acknowledged.*

References

[1] Valiev RZ, Murashkin MY, Sabirov I. A nanostructural design to produce high-strength Al alloys with enhanced electrical conductivity. *Scripta Materialia.* 2014;76: 13-16.

[2] Lewandowska M, Kurzydlowski KJ. Recent development in grain refinement by hydrostatic extrusion. *Journal of Materials Science.* 2008;23-24: 7299-7306.

[3] Braunovic M. Evolution of Different Contact Aid Compounds for Aluminium-to-Copper Connections. *IEEE Transaction CHMT.* 1992;15(2): 216-224.

[4] Association TA. *Aluminium Electrical Conductor Handbook.* 3rd ed. Washington, USA; 1989.

[5] Campbell J. *Castings.* 2nd edition. Oxford, UK: Butterworth-Heinemann; 2003,

[6] Simensen CJ, Berg G. A survey of inclusions in aluminum. *Aluminum.* 1980;56(5): 335-340.

[7] Liu C, Hu Z, Zeng J. Removal of Impurities in Aluminum by Use of Fluxes. *Advanced Materials Research.* 2012;509: 152-155.

[8] Rana RS, Purohit R, Das S. Reviews on the influences of alloying elements on the microstructure and mechanical properties of aluminum alloys and aluminum alloy composites. *International Journal of Scientific and Research Publications.* 2012;2(6): 1-7.

[9] Polmear IJ. *Light Alloys.* 4th Edition, Elsevier, Butterworth-Heinemann, UK; 2005.

[10] Roy RK. Recrystallization Behavior of Commercial Purity Aluminium Alloys. In: Monteiro WA. (ed.). *Light Metal Alloys Applications.* London, UK: IntechOpen; 2014.

[11] Kaiser MS, Datta S, Roychowdhury A, Banerjee MK. Age hardening behaviour of wrought Al-Mg-Sc alloy. *Journal of Materials and Manufacturing Processes*. 2008;23(1): 74-81.

[12] Chester GV, Thellung A. The Law of Wiedemann and Franz. *Proceedings of the Physical Society.* 1961;77(5): 1005-1013.

[13] Holman JP. *Heat Transfer.* 7th edition. Singapore: McGraw-Hill Book Company; 1990.

[14] Jin S. Recent advances in electrically conductive materials. *Journal of Minerals, Metals and Materials.* 1997;49(3): 36-37.

[15] Kaiser MS. Effect of scandium on the softening behaviour of different degree of cold rolled Al-6Mg alloy annealed at different temperature. *International Journal of Advances in Materials Science and Engineering.* 2014;1(1): 39-49.
[16] Omotoyinbo JA, Oladele IO, Shokoya W. Effect of the Degree of Plastic Deformation on the Electrical Resistance and Thermal Conductivity of Al-Mg-Si Alloy. Leonardo Electronic *Journal of Practices and Technologies.* 2014;13(24): 37-50.
[17] Olhoeft GR. Low-frequency electrical properties. *Geophysics.* 1985;50(12): 2492-2503.
[18] Slade PG. *Electrical Contacts, principles and applications.* 2nd edition. Taylor and Francis Group, USA; 2014.
[19] Ahmad HMN, Ghosh S, Dutta G, Maddaus AG, Tsavalas JG, Hollen S, Song E. Effects of Impurities on the Electrochemical Characterization of Liquid-Phase Exfoliated Niobium Diselenide Nanosheets. *The Journal of Physical Chemistry C.* 2019;123(14): 8671-8680.
[20] Matin MA, Hossain MN, Ali MA, Hakim MA, Islam MF. Enhanced dielectric properties of prospective $Bi_{0.85}Gd_{0.15}Fe_{1-x}Cr_xO_3$ multiferroics. *Results in Physics.* 2019;12: 1653-1659.
[21] Koaib J, Bouguila N, Abassi H, Moutia N, Kraini M, Timoumi A, Vazquez CV, Khirounia K, Alaya S, Dielectric and electrical properties of annealed ZnS thin films. The appearance of the OLPT conduction mechanism in chalcogenides. *The Royal Society of Chemistry.* 2020;10: 9549-9562.
[22]. Zhang G, Brannum D, Dong D, Tang L, Allahyarov E, Tang S, Kodweis K, Lee JK, Zhu L, Interfacial Polarization-Induced Loss Mechanisms in Polypropylene/$BaTiO_3$ Nanocomposite Dielectrics. *Chemistry of Materials.* 2016;28: 4646-4660.
[23] Rajesh P, Boopathi K, Ramasamy P. Investigations on the solubility, growth, structural, optical, mechanical, dielectric and SHG behaviour of ammonium acetate doped ammonium dihydrogen phosphate crystals. *Journal of Crystal Growth.* 2011;318: 751-756.
[24] Kaiser MS. Trace impurity effect on the precipitation behaviuor of commercially pure aluminium through repeated melting. *European Journal of Materials Science and Engineering.* 2020;5(1): 37-48.
[25] Yakubu OH, Usman I, Aliyu A, Emmanuel OO. Influence of iron content and plastic deformation on the mechanical properties of 8011-type Al-Fe-Si alloy. *Nigerian Journal of Technology.* 2016;35(1): 122-128.